

Adsorption and Desorption Mechanisms of Methylene Blue Removal with Iron-Oxide Coated Porous Ceramic Filter

Fangwen LI, Xiaoi WU, Songjiang MA, Zhongjian XU, Wenhua LIU, Fen LIU

School of Chemistry and Chemical Engineering, Hunan University of Science and Technology, Xiangtan, China

E-mail: lifangweng1@126.com

Received January 17, 2009; revised March 2, 2009; accepted March 4, 2009

Abstract

Adsorption and desorption mechanisms of methylene blue (MB) removal with iron-oxide coated porous ceramics filter (IOCPCF) were investigated in batch and column mode. The results revealed that MB removal mechanisms included physical adsorption and chemical adsorption, of which chemical adsorption by surface ligand complex reaction played a dominant role after infrared spectrum analysis. Recycling agents were selected from dilute nitric acid (pH=3), sodium hydroxide solution (pH=12) and distilled water. Among three agents, dilute metric acid (pH=3) was the best recycling agent. Regeneration rate of IOCPCF arrived at 82.56% at batch adsorption and regeneration was finished in 75min at column adsorption. Adsorption-desorption cycles of IOCPCF after batch and column adsorption were four and three times, respectively. Further, compared with fresh IOCPCF, MB removal rate with these desorbed IOCPCF adsorption only slightly decreased, which suggested that IOCPCF should be used repeatedly.

Keywords: Iron-Oxide Coated Porous Ceramics Filter, Adsorption, Desorption, Methylene Blue, Surface Complex Reaction, Reuse

1. Introduction

Dyestuff removal was primary problem in the printing and dyeing wastewater treatment. At present, the ways, such as adsorption, chemical oxidation, catalytic oxidation, biological method and membrane method, were often used [1,2]. Thereinto, adsorption could eliminate organic compounds which were resistant to degradation by biological method or general oxidation, for example, nitroaromatics and hetero-cyclic compounds, and it took on advantages such as simple operation, less land occupation, good effect and so on. So, adsorption was widely employed in the printing and dyeing wastewater treatment.

There are two shortcomings in the printing and dyeing wastewater treatment by active carbon, which is commonly used absorbent: 1) Higher disposing cost limits its extensive use; 2) Active carbon shows shielding effect on dyestuff removal because its pore

diameter is smaller than molecular diameter of dye-stuff [3]. So, it is vital that low-cost absorbent should be prepared. For instance, more and more adsorbents from farming byproducts and industrial waste were used in the printing and dyeing wastewater treatment because of their rich resource and lower cost [4,5].

Adsorption includes batch and column adsorption, but column adsorption plays a dominant role in the practical application. In order to reduce treatment cost and improve processing efficiency, the absorbent must be better adsorption and desorption performance. Therefore, batch adsorption, column adsorption and their regeneration for MB removal from aqueous solution were implemented using home-made IOCPCF as a absorbent. Adsorption and desorption mechanisms of MB were emphatically analyzed, which hopes to provide theoretical basis for industrial wastewater treatment by porous ceramics filter.

2. Experiment

2.1. Chemicals

All chemicals and reagents used for experiments and analyses were of analytical grade, such as sodium hydroxide, ferric nitrate, MB. Porous ceramics filter based on red mud was kindly provided by Shandong Aluminium Corporation.

2.2. Methods

According to literature 6, surface modification and related performances test of porous ceramics filter, whose particle size is between 1.0mm and 1.2mm, were made. The MB stock solution was prepared by dissolving accurately weighted MB in distilled water to the concentration of 500mg/L. The experimental solution was obtained by diluting the stock solution in accurate proportions to different initial concentrations.

Batch adsorption experiments were carried out in a constant temperature water bath-vibrator at 150rpm and at an ambient temperature (20–40°C) using 150mL conical flask (having plug) containing 50mL of initial MB concentration (100mg/L) and initial pH (11). The initial pH value of the MB solution was previous adjusted with 0.1N NaOH using a pH meter (PHS-3C, China). The adsorbent (5g) was added to each flask, and then the flasks were sealed up to prevent change of volume of the solution during the experiments. After shaking the flasks for predetermined time intervals, the residual MB solution was sampled and determined. Regeneration rate of IOCPCF was calculated according to as follows: 1) After adsorption equilibrium, average adsorption content (q_1) of IOCPCF was decided; 2) The used adsorbent (5g) was again added to a flask containing 50mL actified solution (one of dilute nitric acid (pH=3), sodium hydroxide solution (pH=12) and distilled water). Then, the flask was shaken for 300min at 30°C. According to forgoing method, the elution amount (q_2) was decided as well; 3) The ratio of q_2 and q_1 was the regeneration rate.

Filtration column was composed of organic glass (1.07cm inner diameter and 75cm in height). An external circulating bath allowed carrying out the experiments at the desired temperature. At the bottom of filtration column, quartz sands were laid as supporting layer whose thickness was 2cm. A separatory funnel (125mL) was set at its top as an elevated water tank, and then flow rate of MB solution could be regulated by control of piston opening of separatory funnel and filtration column. The height of IOCPCF, initial concentration, initial pH and temperature in filtration column were 40cm, 50mg/L, 11 and 30°C, respectively. Regeneration in column adsorption adopted to dilute nitric acid as recycling agent and flow rate at regeneration was 4mL/min. The sampling interval was 15min.

The MB solution concentrations in the supernatant were estimated by measuring absorbance at maximum wavelength ($\lambda_{\max}=663\text{nm}$) with a 721-spectrophotometer (Shanghai, China) and computing from the calibration curves.

3. Results and Discussion

3.1. Adsorption and Desorption in Batch Mode

Figure 1 shows adsorption kinetics on MB removal at 20°C, 30°C and 40°C in batch mode. It was obvious that the removal rate reduce of MB was rapid during the initial stages. Then MB uptake capacities increased with time and reached equilibrium values at approximately 300min for three temperatures. At the same time, MB uptake capacities enhanced from 0.56mg/g to 0.85mg/g with temperature increase from 20°C to 40°C, which suggested that the adsorption was endothermic reaction and higher temperature was propitious to MB removal.

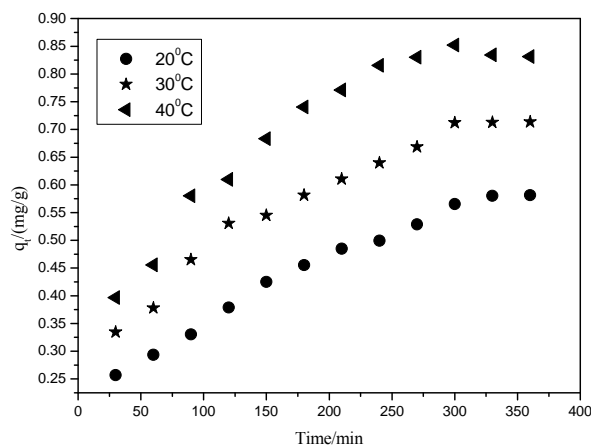


Figure 1. Adsorption kinetic curves at different temperature.

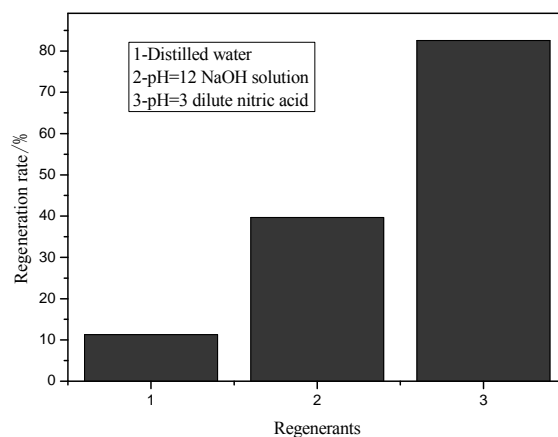


Figure 2. Effect of regenerating agent species on regeneration of IOCPCF.

IOPCPF regeneration after equilibrium at 30°C by three recycling agents is illustrated in Figure 2. It was seen from Figure 2 that regeneration rate of dilute nitric acid (pH=3) was the highest (82.56% or so), next to NaOH (39.67%) and last to distilled water (11.25%).

In order to examine effect of IOPCPF regeneration on MB removal, four adsorption-desorption cycles were made (Figure 3) and recycling agent was dilute nitric acid. As it is shown in Figure 3, MB removal rate was 72.06% with fresh IOPCPF, namely regeneration cycle was zero. However, MB removal rate reduced to 60.87% after four regeneration cycles. This was attributed to the following reasons: IOPCPF could not completely regenerated and iron modification coat of IOPCPF surface had wee loss (0.001622%) during adsorption and desorption because of vibration [6], which led to some adsorption sites reduce. But compared with fresh IOPCPF, the decrease was not significant. It can be inferred that IOPCPF may be regenerated with dilute nitric acid and reused.

3.2. Adsorption and Desorption in Column Mode

Figure 4 shows breakthrough curves at different flow rate. The breakthrough time reduced from 66min to 9min with flow rate increase from 2mL/min to 4mL/min. When flow rate was 8mL/min, the column had been breakthrough from the beginning, which represented that the flow rate (8mL/min) was too high for the column adsorption experiment. The reasons were that contact time was more between MB and IOPCPF at low flow rate. The empty bed residence time (EBRT) was 18, 9 and 4.5min at flow rate 2, 4 and 8mL/min, respectively. MB uptake capacity was 0.078mg/g according to Thomas model [7] at flow rate 8mL/min.

Figure 5 and Figure 6 shows desorption and reuse of adsorption column after breakthrough at flow rate 2mL/min. As shown in Figure 5, MB from saturated IOPCPF was desorbed fast at the beginning. The value of C_t/C_0

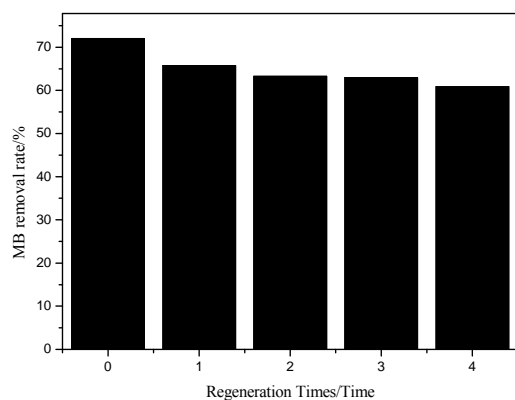


Figure 3. Effect of regeneration cycles on MB removal rate of IOPCPF.

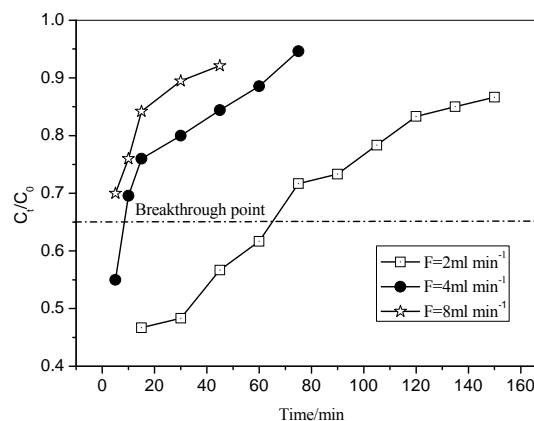


Figure 4. Breakthrough curves for MB adsorption on IOPCPF at different flow rate.

was equal to 40.32%. Next the desorption rate decreased gradually. At last desorption finished after 75min. In Figure 6, MB removal rate had no significant difference between regenerative column and fresh column during the initial and middle operation period, but MB removal decreased prominently at the later operation period. The reasons were ascribed to as the following: a small part of adsorption sites in regenerative column could not regenerate, but regenerative column had enough adsorption sites for MB during the initial and middle operation period. However, inadequate adsorption sites resulted in MB removal rate decrease at the later operation period in regenerative column. Like batch adsorption, compared with fresh IOPCPF, the decrease was not significant. It can be inferred that IOPCPF may be regenerated with dilute nitric acid and reused.

3.3. Adsorption Mechanisms of MB Removal

From batch adsorption study, MB uptake capacities enhanced with temperature increase, which followed the features of chemical adsorption. Moreover, IR (Infrared

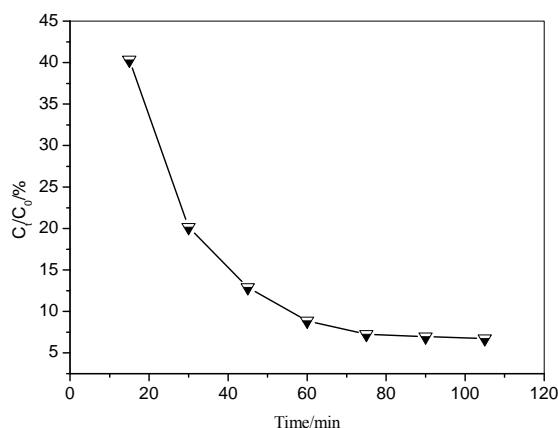


Figure 5. Desorption curve for MB adsorption on IOPCPF.

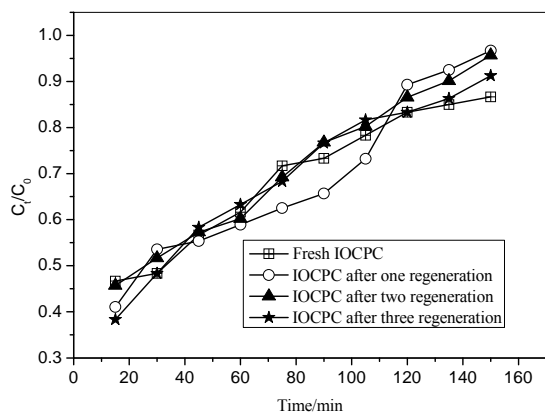


Figure 6. Recycling of regenerative adsorption column.

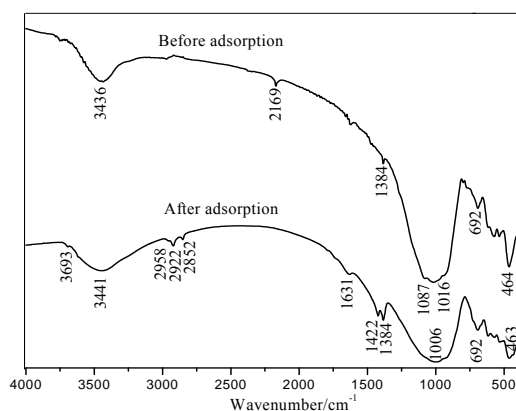


Figure 7. Infrared spectra of IOCPFC before and after adsorbed MB (MB initial concentration: 100mg/L, Temperature: 30°C).

Spectrum) may be used for tracking existed chemical reaction and exploring the reaction mechanism. Figure 7 shows IR curves of IOCPFC before and after batch adsorption.

It could be inferred that chemical bonding between MB and related groups of IOCPFC may take place from Figure 7 based on following facts: 1) After adsorption, the stretching vibration adsorption band of hydroxyl groups at 3441cm⁻¹ was broadening and offset; 2) After adsorp-

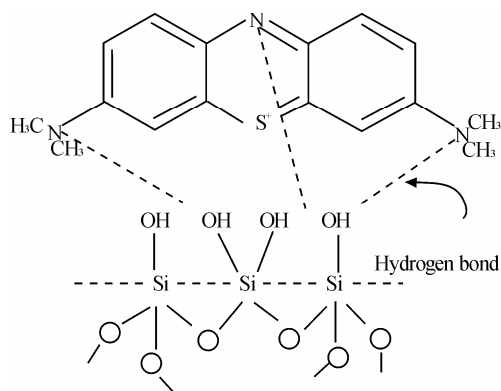


Figure 8. Hydrogen bond formation between adsorbent and MB.

tion, the new stretching vibration adsorption bands at 2800–3000cm⁻¹ and 1422cm⁻¹ were attributed to methyl and benzene ring framework from MB; 3) After adsorption, the adsorption bands of Si-O-Si or Fe-O-Si groups at 1000–1200cm⁻¹ broadened as well.

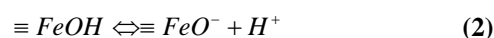
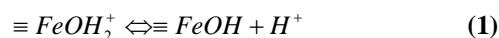
On the basis of above analyses, chemical adsorption of MB happened by the following two chief ways:

1) Surface ligand complex reaction

Based on surface ligand theory, surface ligand complex models between IOCPFC and water interface were cited as the following [8,9]:

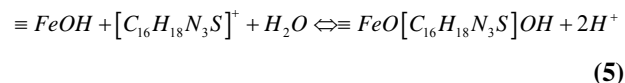
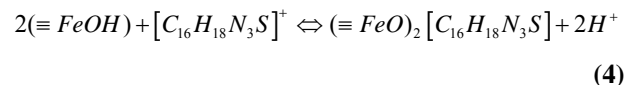
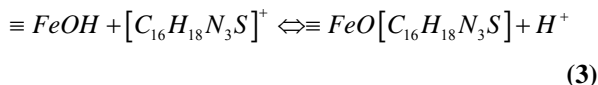
a) The surface protonic ionization reaction

Surface ferric-oxide compounds of IOCPFC existed in aqueous solution in three forms after hydration, i.e., $\equiv FeOH_2^+$, $\equiv FeOH$ and $\equiv FeO^-$, and then they may mutually transform according to following forms:



b) The adsorption of MB cation

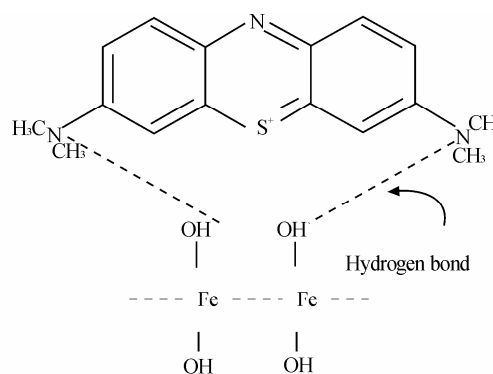
MB existed in aqueous solution in cation ($[C_{16}H_{18}N_3S]^+$) which reacted with the above ferric-oxide compounds by the following forms:



Thus, MB was removed by the formed complex.

2) Hydrogen bond forming

Nitrogen atoms from MB have awful attracting electron ability and less atom radius, so they can form hydrogen bond with hydroxyl groups from IOCPFC surface. Figure 8 explained the hydrogen bond forming process.



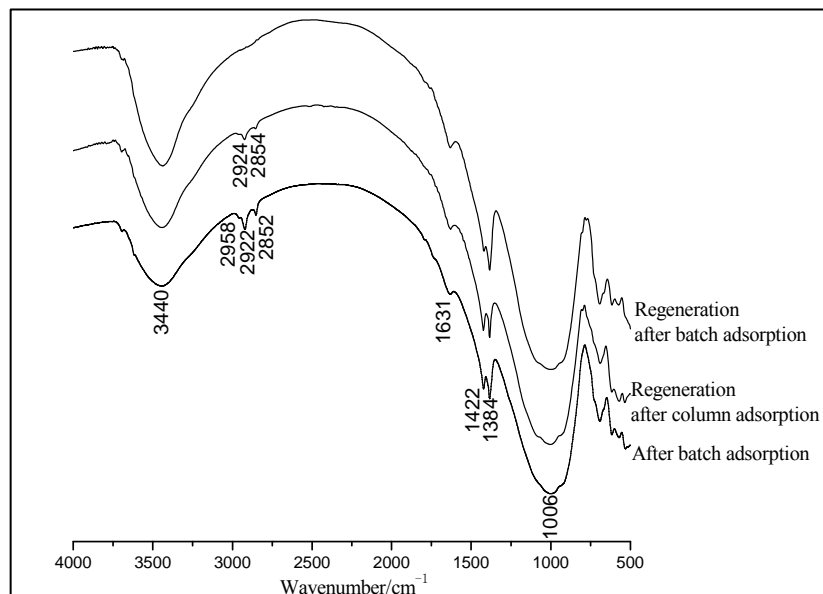


Figure 9. FTIR curves of regeneration of IOPCPF after absorbed MB.

In addition, adsorption isotherms (omitted) of MB presented “S” type rather than “L” type and the adsorption activation energy was 16.1445kJ/mol which was slightly higher than 4.184kJ/mol (physical adsorption), which suggested that physical adsorption, including static adsorption and van der waals force adsorption, was one of mechanisms of MB removal.

3.4. Desorption Mechanisms of MB

Many hydrogen ions in acid medium urged the above equations to move towards the left side, so $[C_{16}H_{18}N_3S]^+$ adsorbed by complex reaction released from IOPCPF surface. Farther, $\equiv FeOH_2^+$ was chief existing form of iron-oxide compounds in acid medium, so $[C_{16}H_{18}N_3S]^+$ was desorbed also by static adsorption.

From Figure 9, it was seen that regeneration of IOPCPF was not complete to both batch adsorption and column adsorption. Comparatively speaking, regeneration effect of batch adsorption was better than that of column because the adsorption bands at 2800–3000 cm^{-1} were no apparent in regeneration IR curve after batch adsorption, but there were these bands, whose intensity decreased in comparison to no regeneration, in regeneration IR curve after column adsorption. At the same time, the adsorption bands at 1422 cm^{-1} were all apparent in both adsorption regeneration IR curves. The MB may be adsorbed by surface ligand complex reaction, whose regeneration need damage chemical bond. In addition, regeneration time of batch adsorption was longer than that of column time.

4. Conclusions

On the basis of the experimental results of this investigation, the following conclusions could be drawn:

- 1) IOPCPF was found to be an effective adsorbent for MB removal.
- 2) Major mechanism of MB adsorption was surface ligand complex reaction between MB and functional groups of IOPCPF surface, and then there were physical adsorption such as static adsorption and van der waals force adsorption also.
- 3) Regeneration of IOPCPF was not complete to both batch adsorption and column adsorption. Comparatively speaking, regeneration effect of batch adsorption was better than that of column.
- 4) Reverse reaction of surface ligand complex reaction and homologous charge repulsion were chief mechanisms of MB desorption.

5. Acknowledgements

We gratefully acknowledge the National Natural Science Foundation of China (Granted No.20577008) and the Doctoral Science Foundation of Hunan University of Science and Technology (Granted No.E58109) for financial support.

6. References

- [1] M. Joonghwan, H. Jeong-Eun, J. Jonggeon, *et al.*, “Pre-treatment of a dyeing wastewater using chemical coagulants,” *Dyes and Pigments*, Vol. 72, No. 2, pp. 240–245, 2007.

- [2] A. P. Pantelis, P. X. Nikolaos, and M. Dionissios, "Treatment of textile dyehouse wastewater by TiO₂ photocatalysis," *Water Research*, Vol. 40, No. 6, pp. 1276–1286, 2006.
- [3] G. M. Walker, "Adsorption of dyes from aqueous solution- the effect of adsorbent pore size distribution and dye aggregation," *Chemical Engineering Journal*, Vol. 83, No. 3, pp. 201–206, 2001.
- [4] G. Renmin, J. Youbin, S. Jin, *et al.*, "Preparation and utilization of rice straw bearing carboxyl groups for removal of basic dyes from aqueous solution," *Dyes and Pigments*, Vol. 76, No. 2, pp. 519–524, 2008.
- [5] H. Runping, W. Yuanfeng, Y. Weihong, *et al.*, "Removal of methylene blue from aqueous solution by chaff in batch mode," *Journal of Hazardous Materials B*, Vol. 137, No. 1, pp. 550–557, 2006.
- [6] F. W. Li, J. F. Wu, X. H. Xu, *et al.*, "Study on surface modification of porous ceramics filter media by iron oxide compound," *Journal of Hunan University of Science & Technology (Natural Science Edition)*, China, Vol. 23, No. 1, pp. 117–120, March 2008.
- [7] H. C. Thomas, "Heterogeneous ion exchange in a flowing system," *Journal of the American Chemical Society*, Vol. 66, pp. 1664–1666, 1944.
- [8] H. Hohl and W. Stumm, "Interaction of Pb²⁺ with hydrous- Al₂O₃," *Journal of Colloid Interface Science*, Vol. 55, No. 2, pp. 281–288, 1976.
- [9] K. F. Hayes and J. O. Leckie, "Modeling ionic strength effects on cation adsorption at hydrous oxide/solution interface I," *Journal of Colloid Interface Science*, Vol. 115, No. 3, pp. 564–572, 1987.